DETERMINATION OF VALANIS MODEL PARAMETERS IN A BOLTED LAP JOINT: EXPERIMENTAL AND NUMERICAL ANALYSIS OF FRICTIONAL DISSIPATION

Authors: J. Abad[a*], F.J. Medel[b], J.M. Franco[c]

Affiliations: [a]Department of Mechanical Engineering. Engineering and Architecture School. University of Zaragoza – I3A (C/ María de Luna s/n, 50018 Spain). javabad@unizar.es

[b]Department of Mechanical Engineering. Engineering and Architecture School. University of Zaragoza. ICMA, CSIC-University of Zaragoza (C/ María de Luna 3, 50018 Spain). fjmedel@unizar.es

[c]Department of Design and Manufacture Engineering. Engineering and Architecture School. University of Zaragoza (C/ María de Luna s/n, 50018 Spain). jfranco@unizar.es

*Corresponding Author: Javier Abad
Department of Mechanical Engineering-I3A
University of Zaragoza
C/María de Luna s/n, Edif. Betancourt, 50018 Zaragoza (Spain)
E-mail: javabad@unizar.es

Abstract

In this work, Valanis model parameters, and their variation with bolt preload, were determined for a bolted lap joint, which consisted in two steel plates held together by a metric 12 screw. For this purpose, a series of transitory non-linear analyses were performed on the basis of a three dimensional finite element model of the bolted lap joint subjected to varying bolt preloads and tangential displacements. Curve fitting of hysteresis cycles obtained from numerical simulations allowed determination of Valanis model parameters as well as assessment of bolt preload influence on these parameters. In addition, the present numerical simulations provided information about the evolution of the contact state from stick to slip regimes between the bolted plates, reflecting the non-linear behaviour of the joint. Quasi-static tests at several preloads and tangential displacements conditions were conducted to validate Valanis model parameters previously obtained from numerical simulations. The present findings provided detailed information about the evolution of the aforementioned Valanis parameters with bolt preload. Thus, we confirmed that equivalent stiffness values corresponding to the macro-slip regime as well as the upper limit of the sticking regime (E_t, and σ_0, respectively) are highly influenced by bolt preload levels. These results may prove useful to appropriately design bolted joints to be used under specific stiffness and damping criteria, and therefore reducing the vibration response of the joint.

Keywords: Bolted lap joint; Equivalent stiffness; Dissipated energy; Valanis parameters; Bolt preload

1. Introduction

Bolted lap joints represent an important component of many structural assemblies used in diverse fields, such as aerospace and automotive industries, or in civil engineering applications [1-3]. These joints are typically preloaded to a constant force value normally applied to the contact surface. The preload is provided by one or more bolts, and, during service, the joint is subjected to fluctuating forces or displacements tangential to the contact surface. The complex phenomenon produced between the contact surfaces of the joint depends on a high number of parameters, being friction coefficient, slip area, and contact pressure the most important [4].

Modelling of friction phenomena in lap joints may be dealt from two different points of view. On one hand, constitutive models may be used, explaining friction on a microscopic basis and relating applied stresses to strains produced. On the other hand, phenomenological models may describe the overall relationship between the friction force and the relative displacement between the contact surfaces. From a phenomenological point of view, bolted lap joints are described by force-displacement curves, which relate tangential forces on the contact surface to the tangential displacement produced between them [5,6]. If a cyclic tangential displacement to certain amplitude is imposed, the registered curve exhibits a distinct hysteresis cycle (Figure 1), where three regimes are clearly differentiated. Thus, when a joint is forced to a tangential displacement, d_T, this firstly behaves in a linear-elastic fashion (Line A-B) since the tangential force on the contact surface, F_T , is below the threshold of relative displacement. This initial behaviour is generally known as sticking. As the tangential displacement increases, a transition region can be observed, the micro-slip region (Line B-C), wherein the area of the contact surface that is slipping is gradually larger. Finally, increasing amplitudes of the tangential displacement provoke bolted lap joints enter into the macro-slip region (Line C-D), wherein the whole contact surface slips. Beyond that point, decreasing tangential displacements result in a sudden switch to a sticking state, reproducing the inverse of the aforementioned phenomenon (Line D-B'-C'-D') [4].

Several studies make use of the hysteresis cycle to determine the stiffness and damping behaviour of individual bolted lap joints to develop dynamic models of the joint within more complex assemblies. Bolted lap joints, when subjected to oscillating tangential forces or displacements, dissipate some energy, E_d, which is equivalent to the area enclosed by the hysteresis cycle (dashed line in Figure 1). This dissipated energy determines the global damping ability of assembled structures and limits the potential harmful effects of resonant vibrations. In addition, the equivalent stiffness, K_{eqv}, of the bolted joint, is determined as the ratio between the force and the maximum tangential displacement produced during the hysteresis cycle and coincides with the slope of line D-D' in Figure 1.

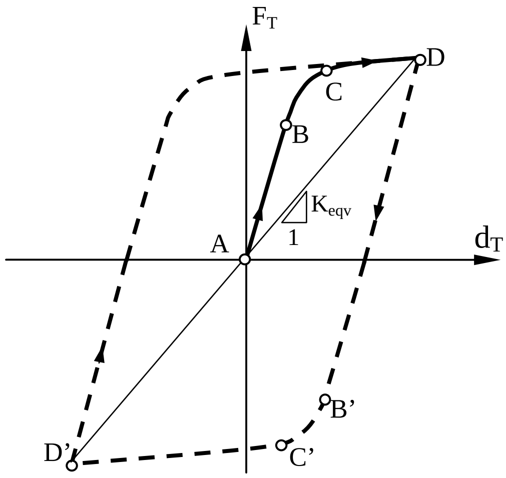

Fig. 1. Typical hysteresis cycle found for a bolted lap joint.

Phenomenological models can be classified in three groups. In the first group, friction force is assumed to be a static function of the relative slip velocity between contact surfaces, being the Coulomb model the most representative. The second group embraces dynamic models, which are based on the evolution of internal state variables. The LuGre model belongs to this second category and was first published in 1995 [7]. Finally, the third group embraces hysteresis friction models, which stem from the elasticity theory to mainly describe energy dissipation and deformation in joints. The Valanis model [8-11] lies in this latter category and it was known and extensively used in the plasticity field. Gaul and Lenz employed the Valanis model to determine the non-linear behaviour of load transfer for a bolted joint, in both micro and macro-slip regimes, and then to simulate the response under cyclic and transitory loads [8,12]. Thus, they succeed in reproducing the experimental results of frictional behaviour of bolted joints. Equation 1 summarizes the Valanis model [8,11]:

$$\dot{F}_T = \frac{E_0 \dot{d}_T \left[1 + \operatorname{sgn}\left(\dot{d}_T\right) \frac{\lambda}{E_0} \left(E_t d_T - F_T \right) \right]}{1 + \kappa \operatorname{sgn}\left(\dot{d}_T\right) \frac{\lambda}{E_0} \left(E_t d_T - F_T \right)} \tag{1}$$

Where E_0 represents the stiffness in the sticking regime, E_t describes the slope of the macro-slip regime, the κ parameter controls the influence of micro-slip, so that high values imply little influence of this regime in joint behaviour, σ_0 establishes the upper limit of the sticking regime, and the λ parameter, which is defined by the following relationship between the former parameters (equation 2):

$$\lambda = \frac{E_0}{\sigma_0 \left(1 - \kappa \frac{E_t}{E_0}\right)} \tag{2}$$

A typical hysteresis cycle based on the Valanis model for a bolted lap joint is shown in Figure 2.

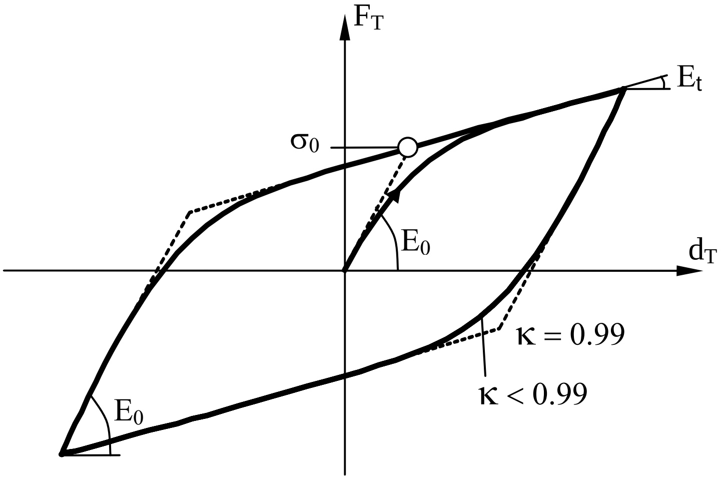

Fig. 2. Valanis model hysteresis cycle for a bolted lap joint

In this work, Valanis model parameters were determined for a lap joint between two steel plates bolted by a metric 12 screw. Analyses of the effects of different preload levels and maximum tangential displacements on the dissipated energy and equivalent stiffness were also conducted. These parameters were determined by fitting hysteresis cycles obtained by means of finite element modelling of the joints. Finite element models also allowed assessment of changes in the contact state of the joint as a function of tangential displacements and bolt preloads. The finite element model results were correlated and validated by experiments on a bolted lap joint subjected to varying tangential displacement amplitudes and bolt preloads.

2. Joint sample

The bolted joint studied in this work corresponds to a bolted lap joint between two steel plates. The joint consists of two steel plates, as well as a M12 bolt, a **not self-locking nut**, and two washers (Fig. 3). **The plates were obtained by means of drilling and milling processes, so that roughness ranged from $R_{a,min}$=1.69µm and $R_{a,max}$=2.49µm (average roughness R_a=1.85µm) as measured by a portable profilometer (Mitutoyo SJ-201) on contact surfaces**. To analyze the behaviour of this joint, varying preload levels, which produced normal pressure onto the contact surface of the two plates, and cyclic tangential displacements were applied. Machining of the two plates was carried out so that the joint surface lied within the medium plane of the plates, thus minimizing bending stresses. **Plates dimensions are shown in Fig. 4, and their geometry was designed so that bending stresses could be avoided. Specifically, the application of the axial force lies into the contact plane, as it is shown in Figure 6, thus minimizing bending. The rest of the components had standard dimensions (Table 1).** The diameter of the holes in plates was 13mm following DIN EN 20273 [13] standard guidelines. This size gives enough space to accommodate bolt movement due to slipping. When the slippage limit is reached, the stiffness of the element is assumed to reach a high value, and therefore the bolted connection would be in a near-rigid state [14,15]. In this work, it is assumed that the displacement experienced by the bolted joint does not exceeds the clearance between the bolt and the hole, as it is common in many civil engineering and machine design applications. Nonetheless, other applications (i.e. aerospace field) use bolted joints with no clearance or even under press-fit conditions [16, 17]. The characteristic material properties for each component are shown in Table 1, with Poisson coefficient ν= 0.3 and longitudinal elastic modulus E = 206 GPa [18, 19].

Table 1. Mechanical properties of the steel parts of the bolted joint

Component	Designation	Material Standard	(Yielding stress) [N/mm^2]	(Tensile strength) [N/mm^2]	(Max. Elongation) [%]
Plate	S355	EN-10025	355	470	17
Bolt	DIN 631 8.8	DIN-ISO 898	640	800	12
Nut	DIN 934 6.8	DIN-ISO 898	480	640	8
Washer	DIN 126 6.8	DIN-ISO 898	480	640	8

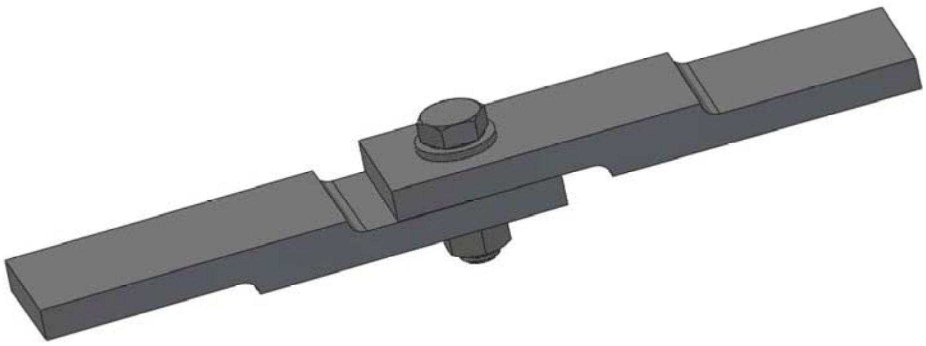

Fig.3. Bolted lap joint

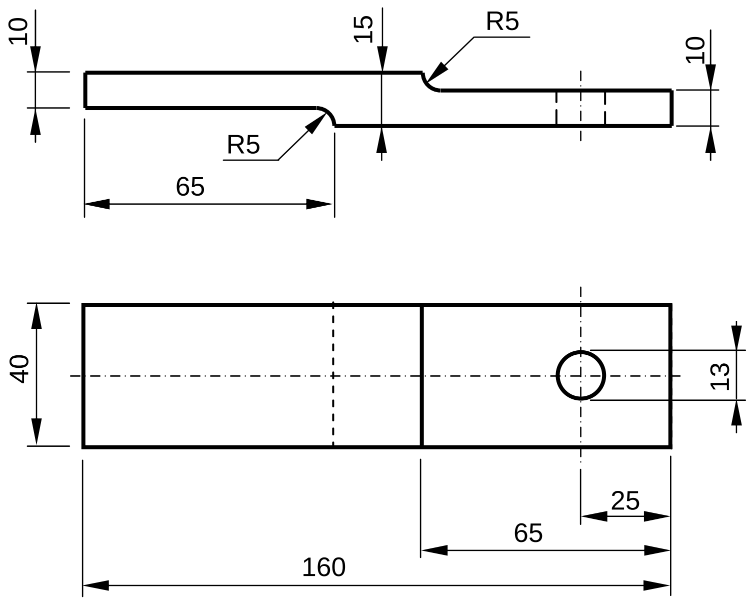

Fig. 4. Plate geometry and dimensions (mm).

3. Experimental analysis

While in some studies [20, 21] bolted joints are subjected to dynamic loads, often at the resonant frequency, in the present work quasi-static experiments were performed to characterize the joint behaviour based on their hysteresis cycles and later correlate them with a finite element model. The quasi-static characterization of bolted joints is a method previously used by other researchers [22, 23]. The main advantage of this methodology is that it closely mimics real-world operation conditions (force levels) for the bolted joint. The experimental testing design allowed easy and expedite characterization of the joint behaviour by means of equipment typically used in mechanical testing.

3.1. Equipment and instrumentation

Experiments were carried out at Instituto Tecnologico de Aragon using a universal testing machine (Instron 8800; Norwood, MA; USA) with dynamic control, hydraulic grip jaws and a maximum force of 100kN. Data acquisition software recorded the applied force and the moving grip jaw displacement.

The application of tightening torque on bolt was made by means of a dynamometric spanner of 30-160 Nm range. The preload force on the bolt was measured with an ALD-W-200 loading cell model (A.L. Trademark; Design Inc.), 0-10000 daN range and 2.14 mV/V sensitivity, connected to a portable bridge of Wheatstone model P3 (Vishay Micro-Measurements Trademark; Malvern, PA; USA) (Fig. 5)

3.2. Assembly and loading conditions

Initially, the plates were placed in the jaws, and they were properly aligned and focused. Then the rest of the components (bolt, loading cell, washer and nut) were placed by applying the tightening torque and registering the preload value in the bolt (Fig. 6).

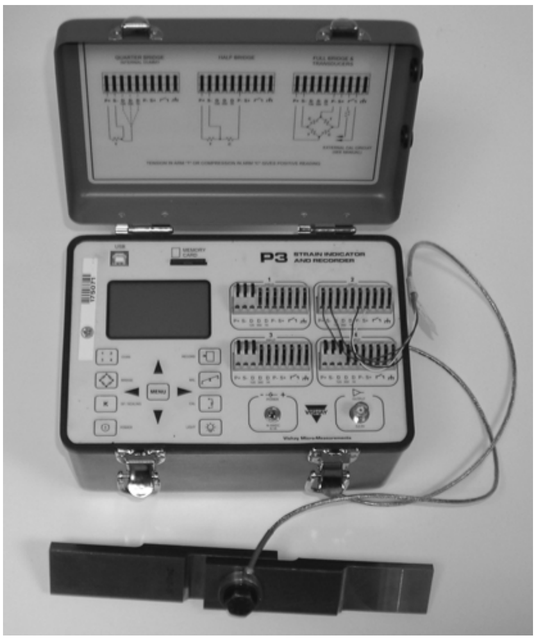

Fig 5. Bolt preload measurement apparatus.

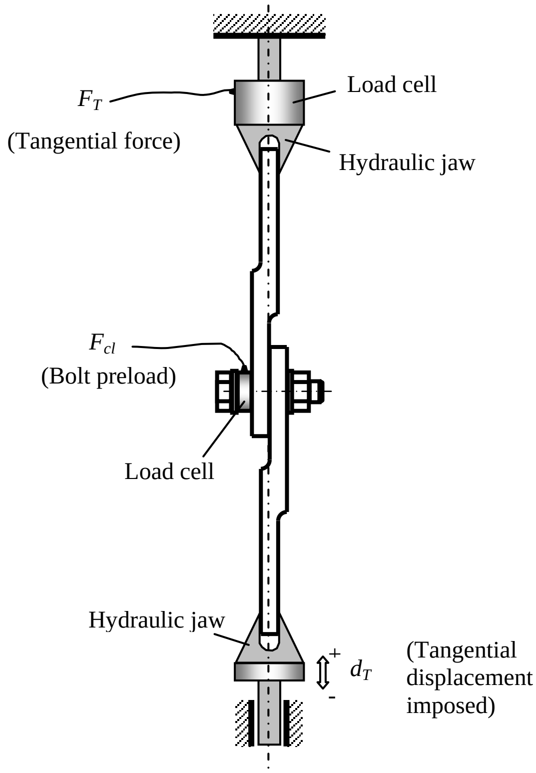

Fig 6. Experimental set-up.

At the free end of the bolted joint, a periodic triangular signal (0.6 Hz) was applied to produce a selected displacement for 10 cycles. A triangular signal was chosen to impose the selected displacements so that the bolted joint was subjected to tangential forces under conditions of constant displacement velocity. Thus, fluctuations between the stick-slip states were avoided. This experiment was repeated to three bolt preload levels and four amplitude displacements as shown in Table 2. Both the imposed displacements and tangential forces were recorded at a 60 Hz sampling frequency. **The magnitude of bolt preload was related to yield strength by means of a β ratio:**

$$\beta = \frac{F_{cl}}{F_y} \tag{3}$$

where F_y is yield strength, and F_{cl} is the applied preload. Yield strength was the maximum force the bolt was able to withstand without suffering plastic deformation in the minor diameter section, A_s, which, in turn, was defined as [24]:

$$A_S = \frac{\pi}{4}(d - 1.3p)^2 \tag{4}$$

where d is the metric diameter, and p represents the thread pitch.

The applied preload was defined as follows [24]:

$$F_{cl} = \frac{T}{Kd_{bolt}} \qquad (5)$$

where F_{cl} is the initial preload (kN), T is the torque (Nm), d_{bolt} is the nominal bolt diameter, and K is the torque coefficient defined as the term which depends on friction coefficients, lead and thread angles, as well as mean diameter of the bolt [25]. A typical value for the torque coefficient is 0.2 [25], however bolt lubrication significantly decreases the friction coefficient of the screw threads allowing higher preloads for the same torque, and therefore smaller torque coefficients, K [26]. In this work, the bolt was lubricated to reduce the scattering between bolt preload and the applied torque, thus obtaining a much more reliable load-torque correlation. Experimental measures carried out during this work confirmed K reached a value of 0.095±4%, which is in good agreement with K values obtained in a previous work by Croccolo and colleagues [26].

Bolt torque maxima were chosen so that the applied preload resulted in bolt preload levels equal to the β=90% [24]). The remaining bolt torque values were selected so that the generated stress levels lie below the aforementioned value, reproducing different joint loosening situations during service. In our work, bolt preload was continuously measured through the whole test, confirming there were no significant variations in this parameter.

Table 2. Imposed bolt preload and maximum tangential displacements used for experimental tests

Test number	β (%) F_{cl} / F_y	Maximum tangential displacement imposed $d_{T,max}$(mm)
1A	57	±0.10
1B		±0.14
1C		±0.18
1D		±0.22
2A	77	±0.10
2B		±0.14
2C		±0.18
2D		±0.22
3A	90	±0.10
3B		±0.14
3C		±0.18
3D		±0.22

3.3. Measurements

Temporal values corresponding to imposed displacements and force levels at the free end of the joint were registered for all the tests included in Table 2. As an example, typical temporal tangential displacements and forces records are shown in Figure 7.

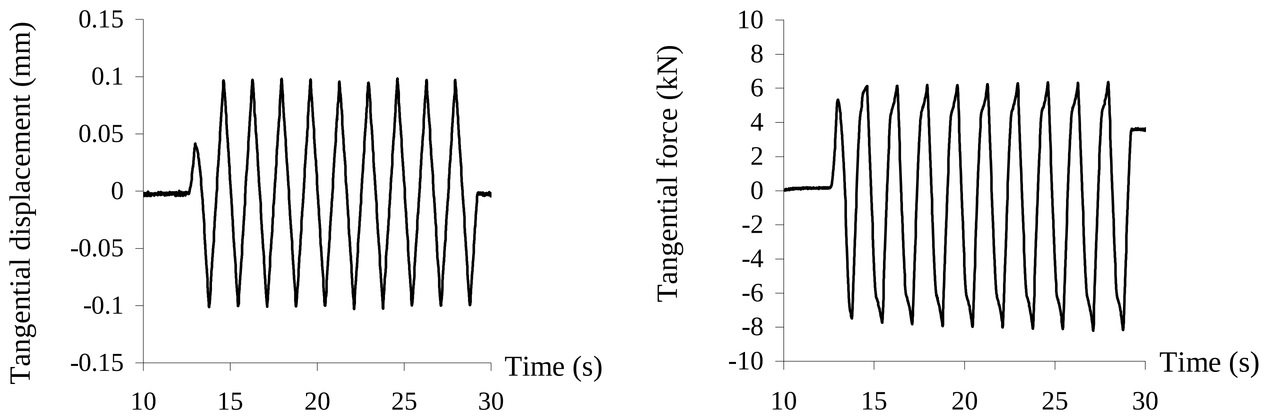

Fig. 7: Temporal displacement and force records corresponding to test 1A

The temporal displacement and force records allowed obtaining hysteresis cycles shown in Fig. 8.

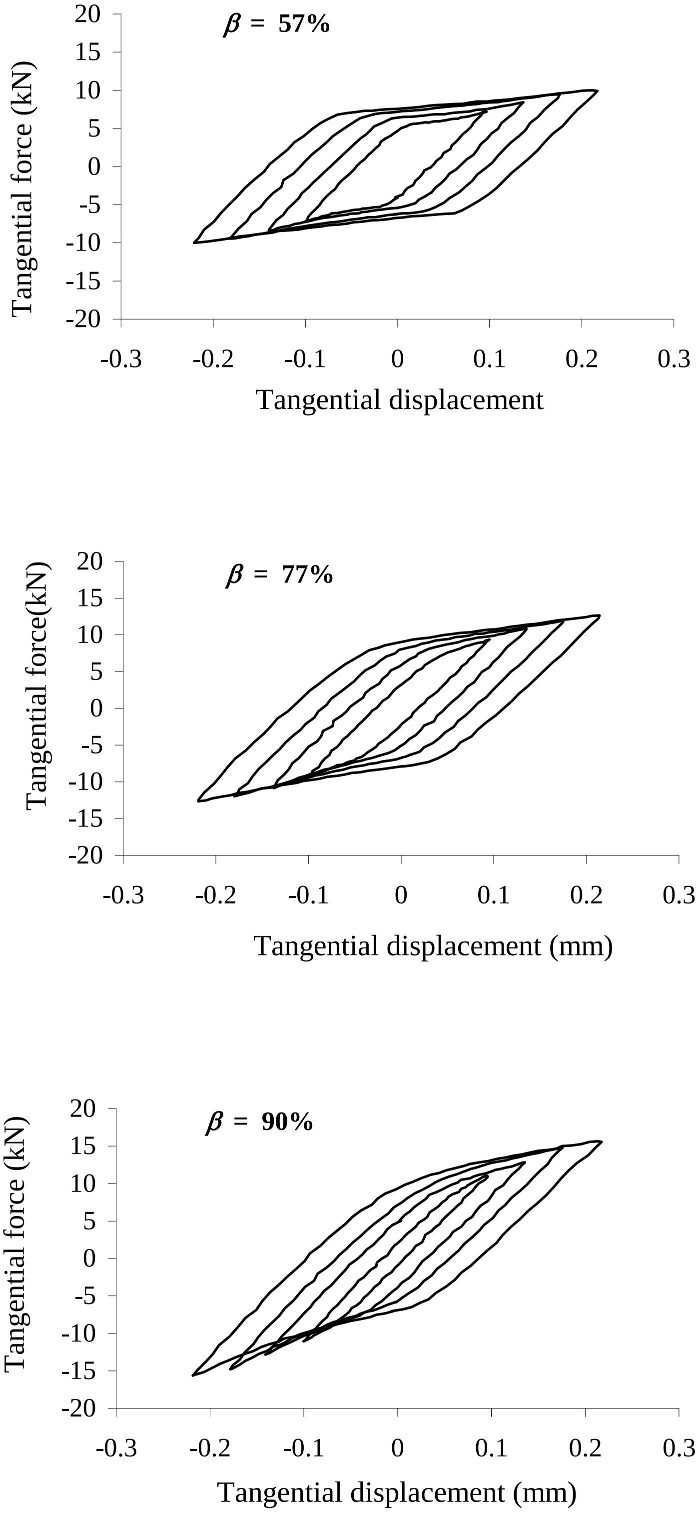

Fig. 8: Hysteresis cycles obtained from temporal force-displacement responses

Finally, dissipated energy and equivalent stiffness parameters were calculated from hysteresis cycles. The first parameter, it was obtained by means of calculations of the area enclosed by the hysteresis cycle and the second one from the maximum force and displacement values.

3.4. Results

To facilitate the analysis of the experimental dissipated energy and equivalent stiffness per cycle, their variation with preload levels and maximum tangential displacement imposed was plotted (Fig. 9).

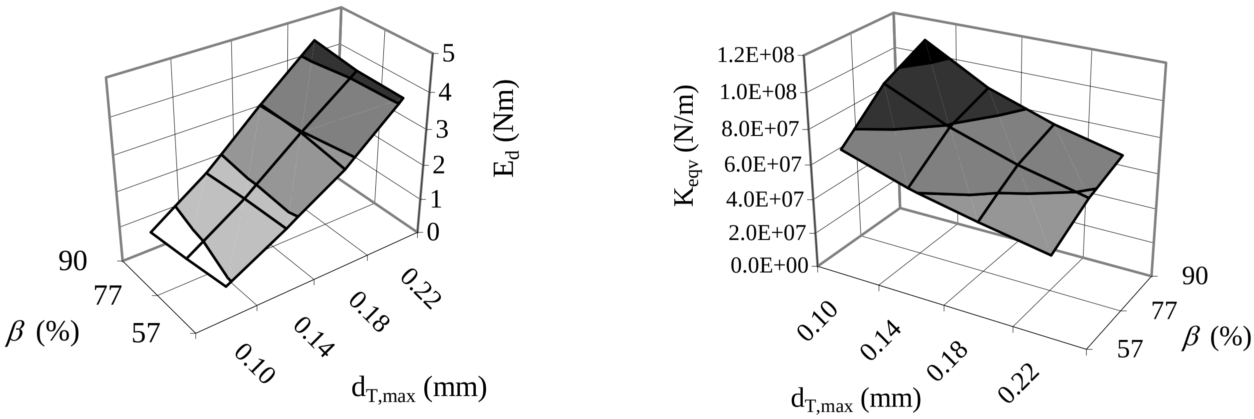

Fig. 9. Response surfaces corresponding to experimental dissipated energy and equivalent stiffness for the bolted joint

It was observed that increasing amplitudes of the imposed displacement resulted in increasingly higher energies dissipated by the joint, while the stiffness decreased. As regards to bolt preload, higher preloads caused an increase in the joint stiffness, and its effect on the dissipated energy was dependent of the imposed displacement. Thus, the dissipated energy decreased at higher preloads for the smaller displacements. A change in this trend was observed over 0.18 mm displacements so that the dissipated energy grew with preload for displacements equal to 0.22 mm or higher.

4. Finite Element Model (FEM) analysis

3D finite element models allow reproduction and characterization of bolted joints behaviour [27-29]. Finite element models, however, are not suitable for dynamic analysis of assemblies including several joints because of too long calculation times. Nevertheless, it is possible to use a quasi-static model to obtain the parameters of a simplified model of the joint, such as those of the Valanis model. In this work, the main purpose of using FEM simulation was to avoid the performance of too many experiments to different preload levels. The FEM provided force-displacement curves for the simulated experiments to selected preload levels, which after proper curve fitting analysis, allowed finding the Valanis model parameters and their relationship to preload. Thus, it was possible to validate the FEM model by comparison with the parameters (dissipated energy and equivalent stiffness) determined from experiments performed to different preload levels.

4.1. Model

A non-linear model of the bolted joint behaviour was developed using ANSYS software. Joint components were meshed using 8 nodes brick elements (SOLID185) [30], with a minimum size of 2.5 mm, giving a model of 7583 elements and 1071 nodes (see Fig. 10). **Mesh size was chosen based on the results of a convergence study performed in one of our previous works [29].**

To model the interaction between components, surface-surface elements (CONTA174 and TARGE170) were employed [31]. The normal interaction between surfaces was described by a penalization method, which allowed surface penetrations of one body into the other controlled by the penalty parameter, the so-called normal contact stiffness or contact stiffness. As for the tangential direction, a Coulomb type friction model established the difference between the sticking and sliding regimes of the joint. In this model, during the sticking-type behaviour shear forces were transmitted without sliding between surfaces, while not exceeding a shear force limit value. Once this limit was exceeded, sliding-type behaviour was produced between both surfaces. Finally, bolt preloads were applied by means of PRETS179 type elements [30], which served to define a pre-stressed section in previously meshed structures.

Details of the finite element model used in the simulation of the joint have been reported elsewhere [29], including a convergence study to determine the appropriate mesh size, as well as the contact parameters. Boundary conditions were modelled introducing an additional pilot node at the lateral sides of the plates, so that all the forces and displacements applied to this node were transferred to the corresponding lateral side. Specific boundary conditions were fixed displacement on one side, and time-periodic displacement on the other. This definition facilitates post-processing since results (reactions and displacements) are referred to a single node and the analysis of energy dissipation in the hysteretic loop is possible by means of force-displacement curves. In summary, the FEM model allowed determination of characteristic force-displacement curves of the joint and calculation of dissipated energy and equivalent stiffness as a function of bolt preloads and maximum tangential displacements imposed to the joint. Numerical results were correlated with experimental findings, thus validating the FEM model used. Likewise, the evolution of the contact state has been studied as a function of the tangential displacement imposed to the joint, as well as the applied bolt preload.

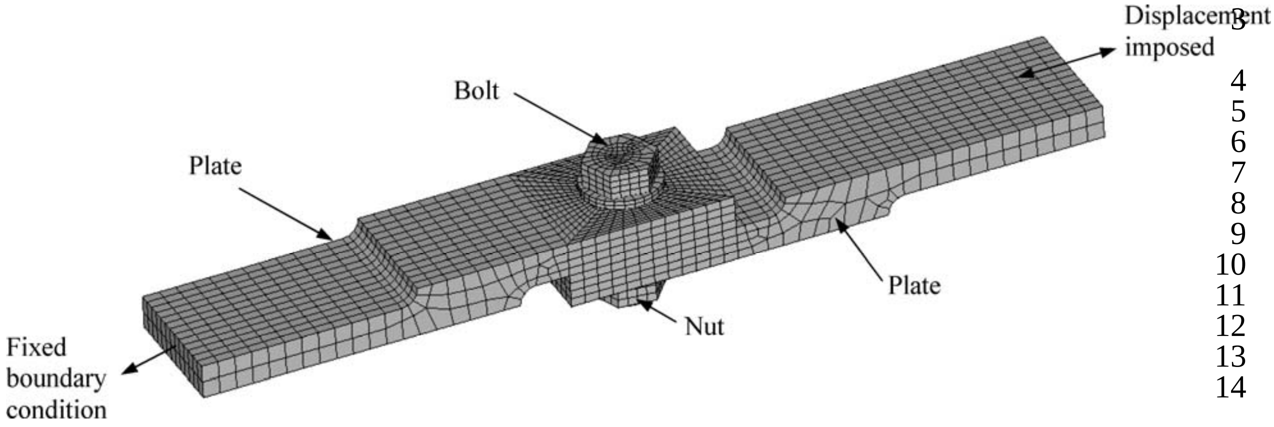

Fig. 10. Meshing of FEM. Parts, loads and boundary conditions are shown

4.2. Results and correlation with experimental data

A total of twenty simulations with ANSYS were carried out [29], with four preload levels **(β=43%, 64%, 85% and 106%)**, five displacement amplitudes (±0.05mm, ±0.10mm, ±0.15mm, ±0.20mm, and±0.25mm) and a static friction coefficient of 0.22. In a previous work [29], the contact parameters of the numerical model, including the static friction coefficient, were found by correlation with the experimental curve for the bolted joint subjected to a monotonic load. **The value of static friction coefficient of 0.22 obtained in the aforementioned work [29] is in agreement with values proposed by other researchers [32, 33].** Response surfaces corresponding to dissipated energy and equivalent stiffness obtained by means of the finite element model are included in Figure 11. It can be observed that the influence of preload and maximum displacement amplitude on the aforementioned parameters was similar to that registered in experimental tests.

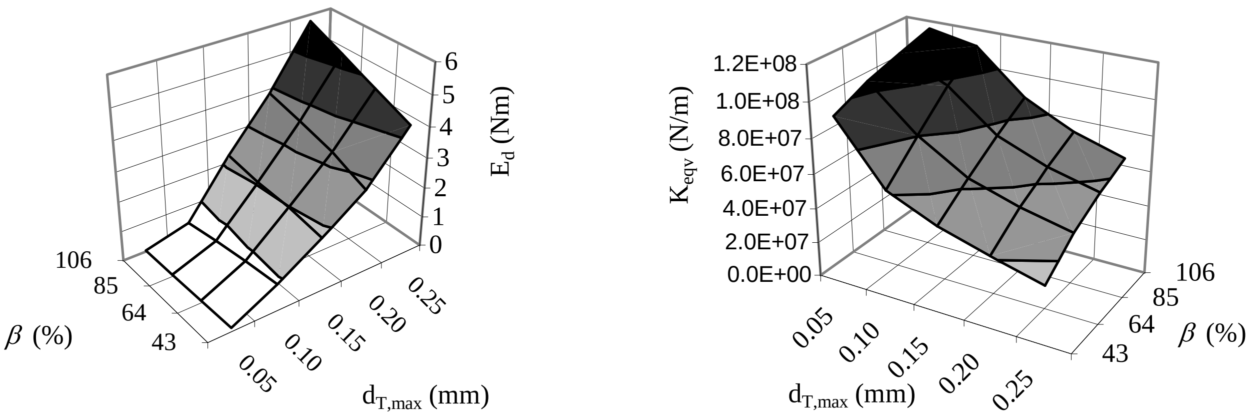

Fig. 11. Response surfaces corresponding to dissipated energy and equivalent stiffness obtained from simulations

To correlate the experimental results with numerical results, the equations of the response surfaces that best fitted the numerical simulations were obtained, applying the Response Surface Methodology (RSM) supported by OPTIMUS software [34,35], and they were used to determine the dissipated energy and equivalent stiffness under the experimental conditions. Correlation results were characterized by maxima errors of about 7 % for the previous parameters, as shown in Table 3.

Table: 3. Numerical-experimental correlation

β (%)	Maximun tangential displacement imposed $d_{T,max}$ (mm)	Energy dissipated per cycle E_d (Nm)			Equivalent stiffness K_{eqv} (N/m)		
		Test	RSM	Error %	Test	RSM	Error %
57	±0.10	0.923	0.857	-7.2	7.32E+07	7.50E+07	2.5
	±0.14	1.807	1.675	-7.3	6.11E+07	6.12E+07	0.0
	±0.18	2.775	2.712	-2.3	5.28E+07	5.32E+07	0.6
	±0.22	4.099	3.928	-4.2	4.57E+07	4.79E+07	4.9
77	±0.10	0.702	0.659	-6.1	9.57E+07	9.22E+07	-3.6
	±0.14	1.74	1.65	-5.2	7.92E+07	7.51E+07	-5.2
	±0.18	2.981	2.801	-6.0	6.72E+07	6.47E+07	-3.8
	±0.22	4.138	4.137	0.0	5.84E+07	5.80E+07	-0.8
90	±0.10	0.516	0.546	5.8	1.08E+08	1.01E+08	-6.5
	±0.14	1.618	1.637	1.2	8.76E+07	8.25E+07	-5.9
	±0.18	3.018	2.912	-3.5	7.46E+07	7.07E+07	-5.3
	±0.22	4.317	4.296	-0.5	6.58E+07	6.34E+07	-3.7

4.3. Evolution of contact condition with tangential displacement

In the initial force-displacement curve obtained by simulation of the joint for a **β=43%** and varying tangential displacement between 0 and a maximum value of 0.2mm, the three regimes previously mentioned, sticking, micro-slip and macro-slip, are clearly differentiated and define the non-linear behaviour of the joint (see Fig. 12).

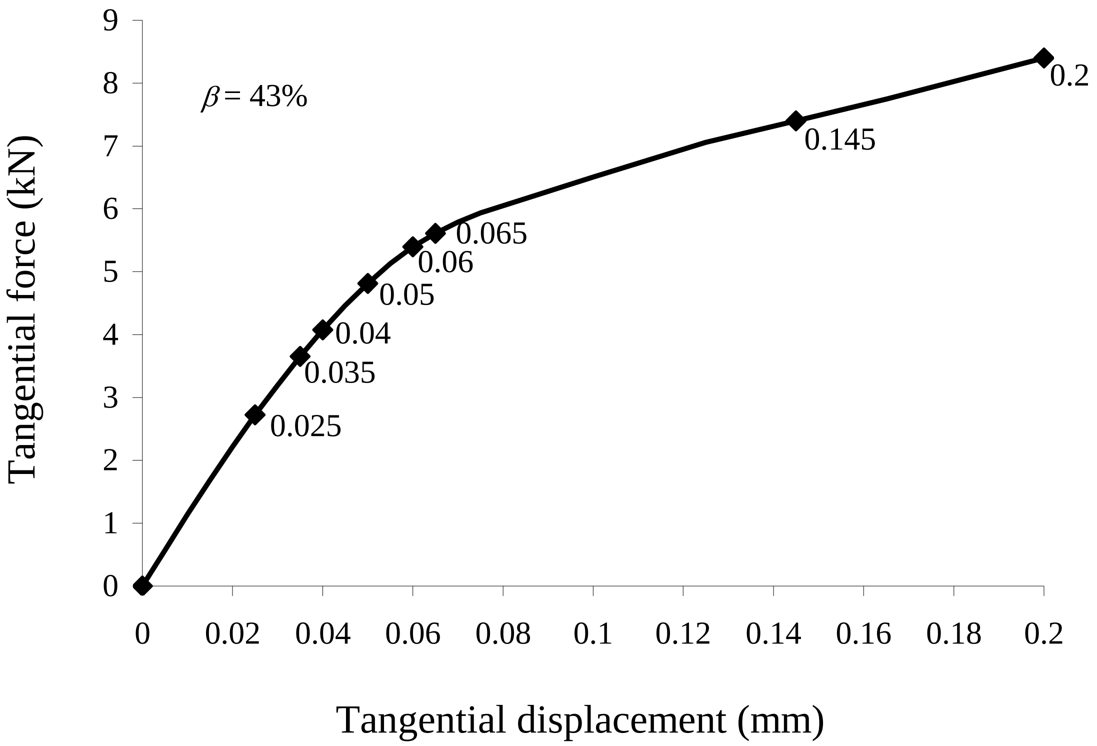

Fig.12. Initial force-displacement curve obtained by simulation

Changes in the force-displacement relationship and the non-linear behaviour are explained by contact state images shown in Figure 13. It can be seen how for the displacement values indicated in Figure 12 the contact state of the interaction surface of the two steel plates gradually evolved from the sticking regime to micro-slip, first, and macro-slip, then, states.

As observed in the first image of Fig. 13, the initial bolt preload generated a contact surface where the contact condition was mostly stick type, situation that holds for displacements lower than d_T=0.025mm (stick behaviour). As the displacement increased, (displacements longer than d_T =0.025mm) the area affected by a stick type contact decreased, whereas the surface with slip type increased (micro-slip behaviour). Finally, a change was produced so that the whole contact surface turned into slip type contact (macro-slip behaviour) for displacements longer than d_T =0.065mm.

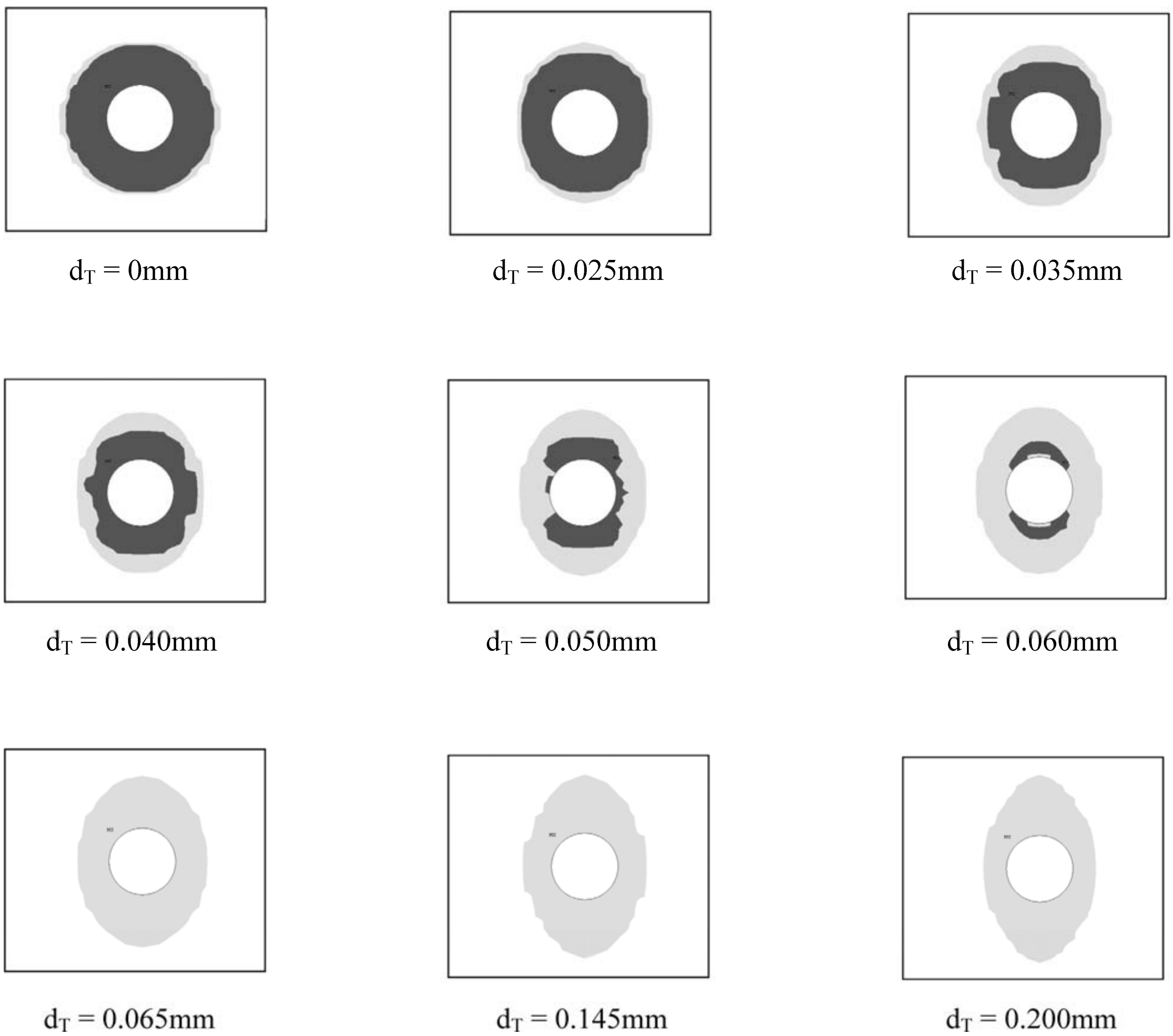

Fig. 13. Evolution of contact condition throughout the range of displacement imposed.

(Dark grey: stick type contact. Light grey: slip type contact)

4.4. Influence of bolt preload on the contact condition

Force-displacement curves were also generated by the present finite element simulations for several initial bolt preloads **(β=43%, 64%, 85%, and 106%)** and tangential displacements (0 – 0.05 mm). These curves presented a similar behaviour for the lower displacements, but they noticeably changed as the imposed displacement increased (see Fig. 14).

The initial bolt preload is a fundamental parameter in the joint behaviour, as it determines the tangential force limit between sticking and slipping regimes on the contact surface. The effect of different initial bolt preloads on the evolution of the contact state of the joint with the tangential displacements imposed is shown in Figure 15.

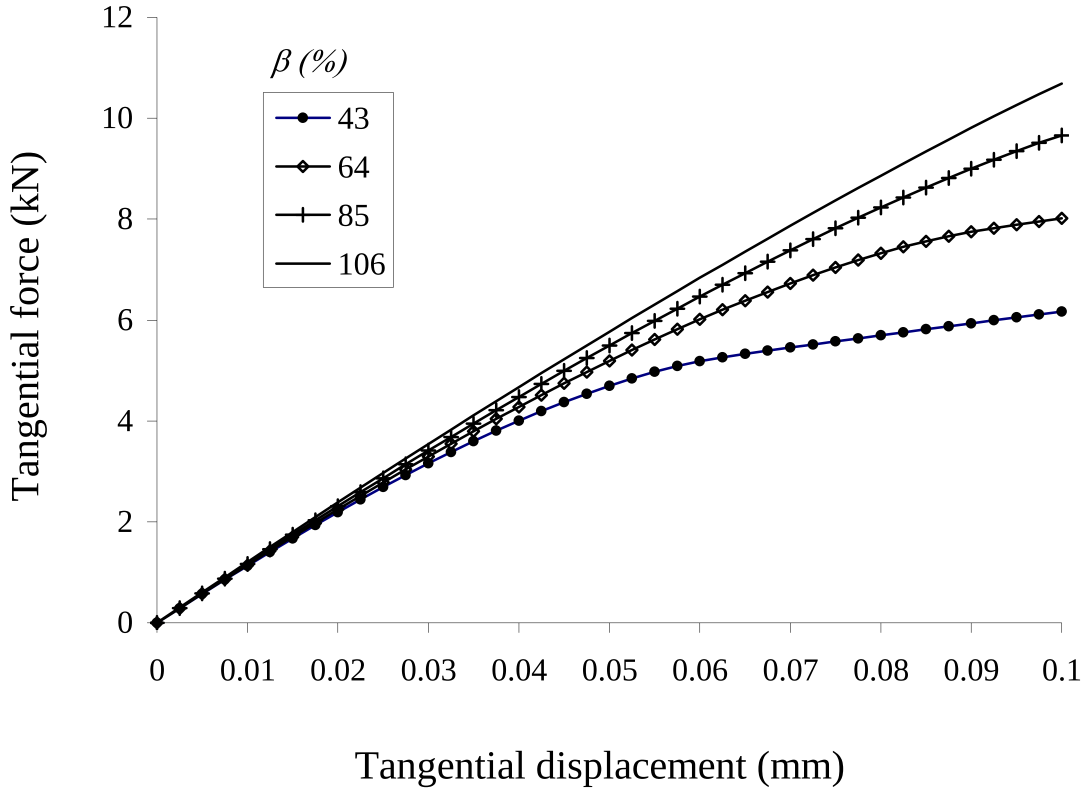

Fig. 14. Initial force-displacement curves obtained by finite element simulations for varying bolt preloads.

Displacements lower than 0.025mm did provoke no significant changes in the contact state regardless of the bolt preload. However, the contact state at maxima tangential displacements was significantly different depending on the bolt preload. Thus, the contact surface in the slip regime became smaller as the bolt preload increased. Whereas at the lowest bolt preload an evolution of the contact state with the displacement amplitude took place, high bolt preloads kept the contact state practically constant. This behaviour can be observed in the curves plotted in Figure 14, where the force-displacement relationship is basically linear and the joint lied into the stick regime for the highest bolt preload. At the lowest bolt preload, however, the force-displacement curve was clearly non-linear, exhibiting both stick and micro slip regions.

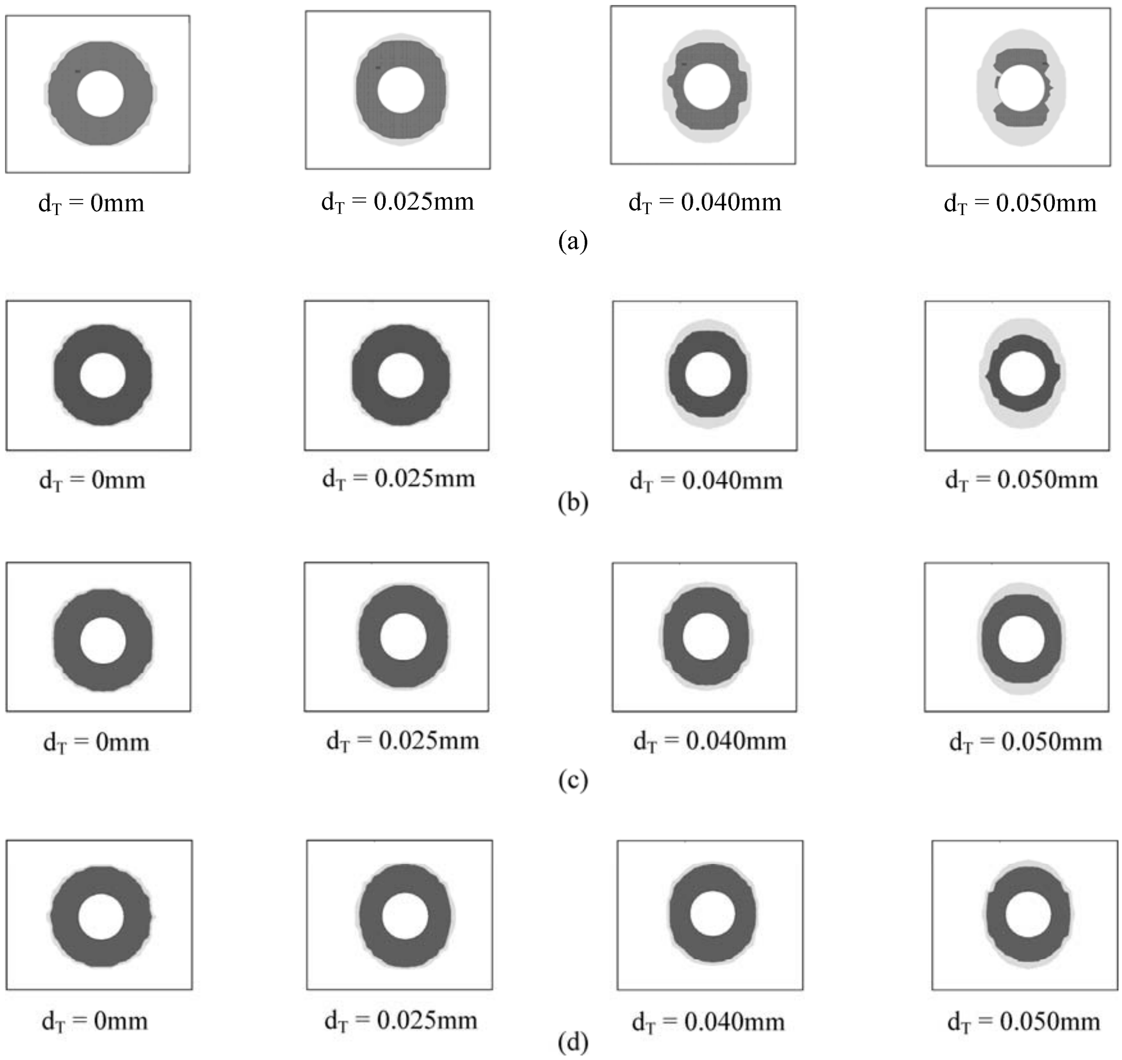

Fig.15. Influence of bolt preload on contact condition evolution (a) **β=43%, (b) β=43%, (c) β=43%, and (d) β=43%**

(Dark grey: stick type contact. Light grey: slip type contact)

5. Valanis model

5.1. Determination of Valanis model parameters obtained from FEM simulations

Curve fitting of the simulated hysteresis cycles (see Fig. 16) served to determine the four Valanis model parameters (see Fig. 17). Analysis of the results shown in Figure 17 revealed the bolt preload had influence on the Valanis model parameters. Thus, bolt preload had little influence in the stiffness of the sticking regime, which corresponds to E_0. On the contrary, the stiffness of the macro-slip regime, which corresponds to E_t, was highly influenced by the preload level. **σ_0 linearly increased for higher bolt preloads, whereas κ was almost constant (0.8) for the bolt preload range explored.**

To quantify the Valanis model parameters dependence on the bolt preload, linear regression equations were generated for the four Valanis model parameters (see Figure 17).

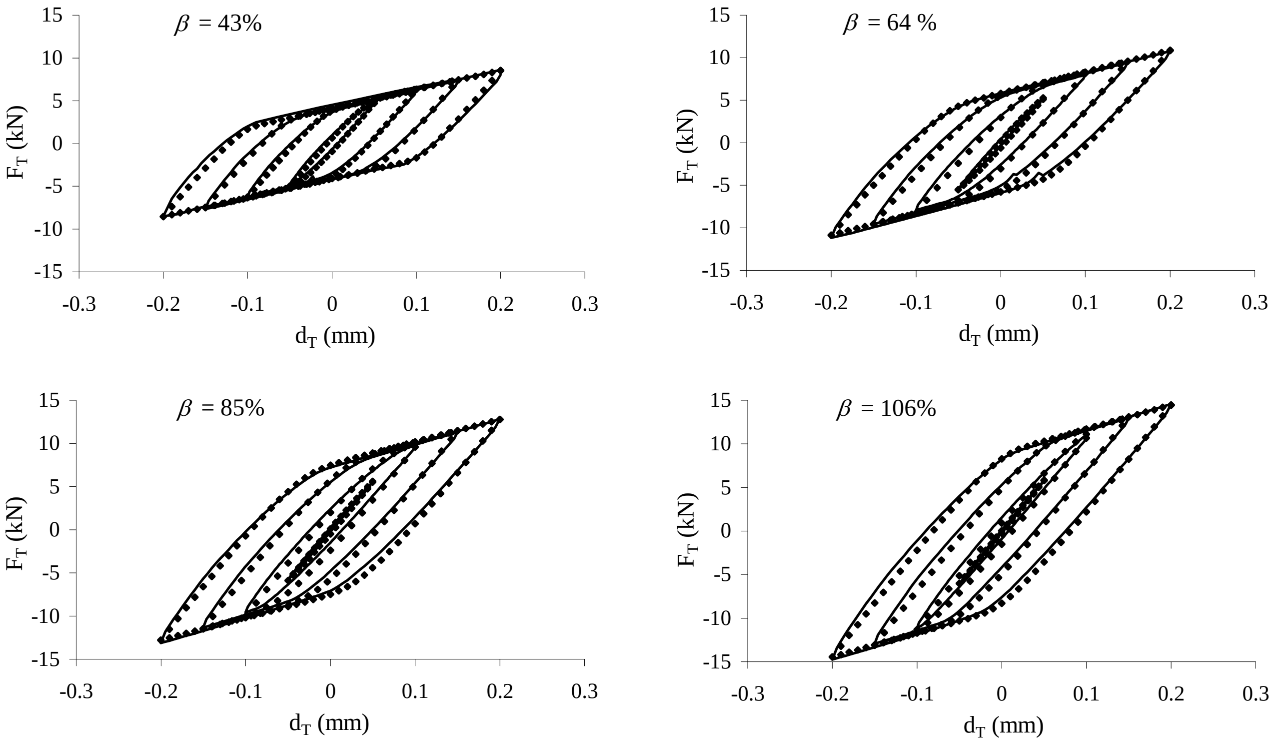

Fig. 16. Simulated hysteresis cycles (—) and Valanis model hysteresis cycles (♦), at different preload levels

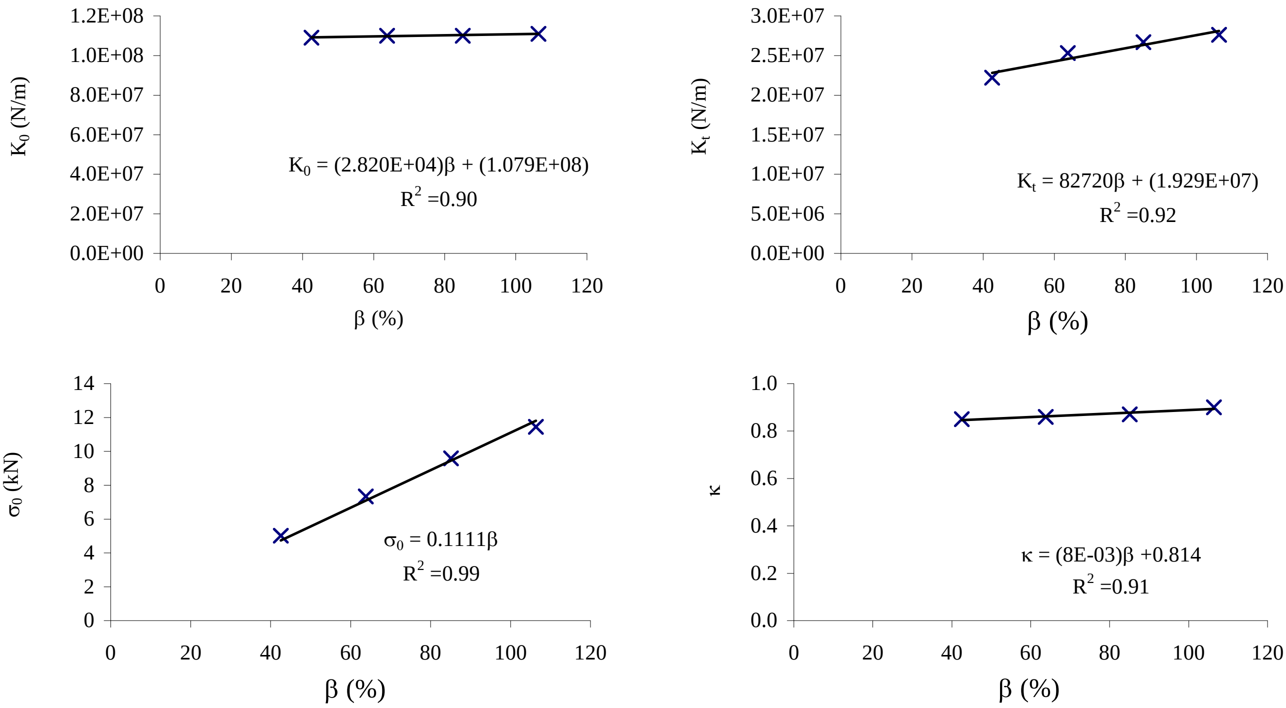

Fig. 17. Linear regression fits (—) for Valanis model parameters (×) at different bolt preloads.

5.2. Validation of Valanis model parameters obtained from FEM simulations

To validate the results of FEM simulations of the bolted joint, the Valanis model parameters (and their associated linear regression equations) corresponding to simulations to different bolt preloads (**β=43%, 64%, 85% and 106%**) were used. The linear regression equations allowed determination of Valanis model parameters for the present experimental bolt preload conditions. Dissipated energy and equivalent stiffness found by means of the analytic Valanis model were confirmed to accurately reproduce the experimental data obtained for the bolted joint (Table 4).

Table: 4. Valanis model-experimental correlation

β (%)	Maximun tangential displacement imposed $d_{T,max}$ (mm)	Energy dissipated per cycle E_d (Nm)			Equivalent stiffness K_{eqv} (N/m)		
		Test	Valanis model	Error %	Test	Valanis model	Error %
57	±0.10	0.923	0.851	-7.8	7.32E+07	7.63E+07	4.2
	±0.14	1.807	1.728	-4.4	6.11E+07	6.15E+07	0.7
	±0.18	2.775	2.586	-6.8	5.28E+07	5.34E+07	1.1
	±0.22	4.099	4.012	-2.1	4.57E+07	4.81E+07	5.3
77	±0.10	0.702	0.648	-7.7	9.57E+07	9.16E+07	-4.3
	±0.14	1.74	1.679	-3.5	7.92E+07	7.32E+07	-7.6
	±0.18	2.981	2.764	-7.3	6.72E+07	6.28E+07	-6.5
	±0.22	4.138	4.012	-3.0	5.84E+07	5.61E+07	-3.9
90	±0.10	0.516	0.557	7.9	1.08E+08	1.02E+08	-5.6
	±0.14	1.618	1.722	6.4	8.76E+07	8.12E+07	-7.3
	±0.18	3.018	2.963	-1.8	7.46E+07	6.93E+07	-7.1
	±0.22	4.317	4.217	-2.3	6.58E+07	6.16E+07	-6.4

6. Conclusions

In this work, an experimental study of the quasi-static frictional behaviour of a bolted lap joint between two steel plates was carried out for different preload levels and imposed tangential displacements, giving a total of twelve experiments. Dissipated energy and equivalent stiffness per cycle were also obtained from the force-displacement hysteresis cycles of the joint. These results were correlated with numerical simulations, proving the suitability of the finite element model in reproducing the frictional behaviour of the joint. This model was later used to determine the Valanis model parameters of the bolted joint studied. In addition, the numerical model served to better understand the non-linear behaviour of the joint, based on the contact surface states between the two steel plates as a function of the tangential displacement and the bolt preload of the joint. Finally, the Valanis model of the bolted lap joint was validated by comparison of the simulation and experimental results.

The findings of this study confirmed that the present bolted lap joint exhibited a non-linear behaviour, which was dependent of preload levels and tangential displacement amplitudes. Variations in preload levels and tangential displacements were also confirmed to determine the evolution of the contact state between stick, micro-slip and macro-slip regimes for the contact surfaces of the bolted plates.

We observed that the bolted joint presented a hysteretic force-displacement behaviour, thus validating the use of the Valanis analytical model. As for the influence of bolt preload levels, we observed that the equivalent stiffness of the joint increased with increasing preloads. The variation of the dissipated energy with bolt preload, however, was dependent of the magnitude of the imposed tangential displacement. Thus, for low tangential displacements, gradually higher bolt preloads implied decreasing dissipated energies, whereas this trend was the opposite for high tangential displacements as dissipated energies increased with increasing preload levels.

The use of a 3D finite element model of the bolted joint allowed us to find appropriate Valanis model parameters, as validated by experimental results. These numerical results also provided the evolution of the aforementioned Valanis parameters with bolt preload. In this sense, we confirmed that equivalent stiffness values corresponding to the macro-slip regime as well as the upper limit of the sticking regime (i.e. E_t, and σ_0) are highly influenced by bolt preload levels. These results may prove useful in appropriate designs of the bolted joint under stiffness and damping criteria, thus limiting the vibration response of the joint.

7. Acknowledgments

This work has been funded with project MYCT/FEDER Ref. BIA2006-15266-C02-02, and by Diputación General de Aragón.

References

[1] Law SS, Wub ZM, Chan SL, Joint Vibration control study of a suspension footbridge using hybrid slotted bolted connection elements, Engineering Structures. 26 (2004) 107-116.

[2] De Benedetti M, Garofalo G, Zumpano M, Barboni R, On the damping effect due to bolted junctions in space structures subjected to pyro-shock, Acta Astronautica. 60 (2007) 947-956.

[3] J.L. Zapico-Valle, J. Abad-Blasco, M.P. González-Martínez, J.M. Franco-Gimeno, M. García-Diéguez, Modelling and calibration of a beam-column joint based on modal data, Computers & Structures. (2012) DOI: 10.1016/j.compstruc.2012.02.016.

[4] M. Eriten, A.A. Polycarpou, L.A. Bergman, Effects of surface roughness and lubrication on the early stages of fretting of mechanical lap joints, Wear. 271 (2011) 2928-2939.

[5] U. Olofsson, Cyclic micro-slip under unlubricated conditions, Tribology International. 28 (1995) 207-217.

[6] S. Bograd, P.Reuss, A.Schmidt, L.Gaul, M.Mayer, Modeling the dynamics of mechanical joints, Mechanical Systems and Signal Processing. 25 (2011) 2801-2826.

[7] C. C. Wit, H. Olsson, K. Aström, P. Lischinsky, A New Model for Control of Systems with Friction, IEEE Transactions on Automatic Control. 40 (1995) 419-425.

[8] K.C. Valanis. Fundamental consequences of a new intrinsic time measure plasticity as a limit of the endochronic theory. National Science Foundation, Washington, D.C. 1978

[9] B. D. Nguyen, Modeling of frictional contact conditions in structures, PhD. Thesis, Georgia Institute of Technology, Georgia, USA, 2005.

[10] H. Ahmadian, H. Jalali, F. Pourahmadian, Nonlinear model identification of a frictional contact support, Mechanical Systems and Signal Processing. 24 (2010) 2844-2854.

[11] H. Jalali, H. Ahmadian, F. Pourahmadian, Identification of micro-vibro-impacts at boundary condition of a nonlinear beam, Mechanical Systems and Signal Processing. 25 (2011) 1073-1085.

[12] L. Gaul, J. Lenz, Nonlinear dynamics of structures assembled by bolted joints, Acta Mechanica, 125 (1997) 169–181.

[13] DIN EN 20273, Fasteners; clearance holes for bolts and screws, 1992

[14] Dennis Göge, Michael Sinapius, Ulrich Füllekrug, Michael Link, Detection and description of non-linear phenomena in experimental modal analysis via linearity plots, International Journal of Non-Linear Mechanics, 40 (2005) 27-48.

[15] S.S. Law, Z.M. Wu, S.L. Chan, Vibration control study of a suspension footbridge using hybrid slotted bolted connection elements, Engineering Structures, 26 (2004) 107-116.

[16] R.H. Oskouei, T.N. Chakherlou, Reduction in clamping force due to applied longitudinal load to aerospace structural bolted plates, Aerospace Science and Technology, 13 (2009) 325-330.

[17] T.N. Chakherlou, Babak Abazadeh, Investigating clamping force variations in Al2024-T3 interference fitted bolted joints under static and cyclic loading, Materials & Design, 37 (2012) 128-136.

[18] EN 10025. Part 2: Non-alloy structural steels. 2004.

[19] DIN-ISO 898. Mechanical Properties of Fasteners. 1999.

[20] H. Ouyang, M.J. Oldfield, J.E. Mottershead, Experimental and theoretical Studies of a bolted Joint excited by a torsional dynamic load, International Journal of Mechanical Sciences, 48 (2006) 1447-1455.

[21] H. Ahmadian, H. Jalali, Identification of bolted lap joints parameters in assembled structures, Mechanical Systems and Signal Processing, 21 (2007) 1041-1050.

[22] M. Eriten, A.A. Polycarpou, L.A. Bergman, Effects of surface roughness and lubrication on the early stages of fretting of mechanical lap joints, Wear, 271 (2011) 2928-2939.

[23] J.F Ferrero, E Yettou, J.J Barrau, S Rivallant, Analysis of a dry friction problem under small displacements: application to a bolted joint, Wear, 256 (2004) 1135-1143.

[24] Bickford J H, An Introduction to the Design and Behavior of Bolted Joints, 3rd ed. New York; Mercel Dekker Inc.; 1995.

[25] R.H. Oskouei, T.N. Chakherlou, Reduction in clamping force due to applied longitudinal load to aerospace structural bolted plates, Aerospace Science and Technology, 13 (2009) 325-330.

[26] D. Croccolo, M. De Agostinis, N. Vincenzi, Failure analysis of bolted joints: Effect of friction coefficients in torque–preloading relationship, Engineering Failure Analysis, 18 (2011) 364-373.

[27] J. Reid, N. Hiser, Detailed modelling of bolted joints with slippage, Finite Elements in Analysis and Design. 41 (2005) 547-562.

[28] J. Kim, J.C. Kang, B.S. Kang, Finite element analysis and modeling os structure with bolted joints, Applied Mathematical Modelling. 31 (2007) 895-911.

[29] J. Abad, J.M. Franco, R. Celorrio, L. Lezáun, Design of experiments and energy dissipation analysis for a contact mechanics 3D model of frictional bolted lap joints, Advances in Engineering Software. 45 (2012) 42-53.

[30] ANSYS Release 10.0 Documentation, Element Reference, ANSYS Inc., 2005

[31] ANSYS Release 10.0 Documentation, Contact Tecnology Guide, ANSYS Inc., 2005.

[32] D.W. Lobitz, D.L. Gregory, D.O. Smallwood, Comparison of finite element predictions to measurements from the Sandia microslip experiment, in: Proceedings of International Modal Analysis Conference, Orlando, FL, 2001.

[33] I.A. Rashquinha, D.P. Hess, Modelling nonlinear dynamics of bolted assemblies, Applied Mathematical Modelling, 21 (1997) 801-810.

[34]OPTIMUS Release 5.2 Documentation, Theoretical Background, Noesis Solutions N.V. Inc., 2006.

[35] Zaiwei Li, Xinhua Liang, Vibro-acoustic analysis and optimization of damping structure with Response Surface Method, Materials & Design. 28 (2007) 1999-2007.